







# Control Loop Based Dimensional Error Compensation for Milling of Near-Net-Shaped, Thin-Walled Structures

Lasse Evers<sup>1</sup> (✉) , Matthias Müller<sup>2</sup>, Carsten Möller<sup>1</sup> , Alexander Brouschkin<sup>1</sup> , and Jan H. Dege<sup>1</sup> 

<sup>1</sup> Institute of Production Management and Technologie (IPMT), Hamburg University of Technologie (TUHH), Denickestr. 17, 21073 Hamburg, Germany

lasse.evers@tuhh.de

<sup>2</sup> FOOKE GmbH, Raiffeisenstraße 22, 46325 Borken, Germany

**Abstract.** Additive manufacturing has the potential to save resources in the production of lightweight aerospace structural components made of Ti-6Al-4V. Currently, these components are milled out of plate-material, resulting in up to 95% of the material being converted into chips that can only be downcycled. However, machining near-net-shape parts poses new challenges. For example, commonly used methods such as the “waterline”- path approach, which uses the residual stiffness of the plate-material to reduce the deflection of the thin-walls due to process forces, can no longer be applied. In this paper, a dimensional error compensation method is presented, that measures the deflection of the workpiece during helical end mill finishing using eddy current sensors. The sensor values are used within a control loop to adjust the toolpaths width of cut and inclination in real time to minimize dimensional error. Next to adjusting for different compliant states of the workpiece, this method adjusts for increasing tool wear states, that produce higher process forces and thereby larger dimensional errors. The presented compensation is compared to a conventional machining approach to demonstrate its capability to enable finishing of near-net-shape parts within tight tolerances while maintaining high material removal rates.

**Keywords:** milling · thin-wall machining · deflection · additive manufacturing · control loop · energy and resource efficiency · waste reduction

## 1 Introduction

Aerospace structural components made of Ti-6Al-4V are typically machined from plate-material, resulting in up to 95% of the material being converted into chips [1]. These chips, contaminated by cooling lubricants and coated with an oxide layer, are unsuitable for economic recycling and reuse in safety-critical structural components, thereby impeding a circular economy [2]. Additive manufacturing (AM), with its near-net-shape forming capability, presents significant potential for reducing the ecological footprint of this manufacturing process by minimizing the material that needs to be machined. However,

components produced through AM fail to meet aerospace tolerances due to their inhomogeneous surfaces, necessitating processing through various methods, including helical milling [3]. Machining near-net-shaped, thin-walled parts introduces new challenges. Process forces during machining can deflect the components, leading to excess material and dimensional errors [4]. Traditional cutting strategies, such as the “waterline”-path approach, rely on the residual stiffness of the plate-material to mitigate deflection and are consequently no longer viable [5]. Therefore, innovative strategies are essential to achieve the necessary dimensional accuracy.

One common method to reduce process forces is to optimize engagement parameters [6, 7]. However, this method has limited effectiveness without compromising productivity, rendering the process less economical compared to conventional machining. In some cases, if components are too compliant, machining becomes impossible. Without new strategies, the significant CO<sub>2</sub> reduction potential of AM remains untapped. Current research is exploring the adaptation of tool paths to the flexibility of the components [6]. Based on expected dimensional errors, the tool is given an additional width of cut  $a_e$  or inclination  $\xi$  to compensate for the workpiece deformation. These additional engagements are determined in advance through simulations, analytical calculation or experiments [6, 8–11]. However, these approaches are time-consuming, require qualified personnel, and do not account for variable factors such as tool wear, making the true deformation prediction difficult [6].

This paper therefore presents an alternative method to achieve the required tool path. The deflection is measured using eddy current sensors, which are used within a control loop to adjust the tool path in real time in order to keep a constant sensor-workpiece distance and minimize the dimensional error.

## 2 Methods

To achieve an automatic process that continuously adapts to varying parameters such as workpiece stiffness and tool-condition-dependent process forces to avoid pre-calculation, the system must directly measure the current deflection. For this purpose, two Micro-Epsilon ES-S2 eddy current sensors connected to eddyNCDT 3060 measurement modules are moved along the thin-wall on the side opposite to the tool. Thereby, they record the workpiece deflection as closely as possible to the final contour-generating point. The sensor values  $\Delta S1$  and  $\Delta S2$  are fed into the 5-axis machining center and converted into a G-Code usable variable. This variable serves as a feedback path for the control loop, as illustrated in Fig. 1. The loop is implemented as a PI-controller via synchronous actions in Siemens Sinumerik 840D sl, operating at an IPO-cycle of  $t_{IPO} = 2$  ms in real time. Desired sensor values  $R_{\Delta S1}$  and  $R_{\Delta S2}$ , representing the target distance between the sensors and the thin-wall, must be input as a reference beforehand. A translational axis and a rotational axis of the machining center are the controlled system of the control loop - in this use case the translational Y-Axis and rotational A-axis. Using these actuators allows for compensation of both displacement and inclination to achieve the desired sensor distances  $R_{\Delta S}$ . Using this method, the tool engagement condition should be continuously maintained and thereby compensate for thin-wall deflection due to process forces.

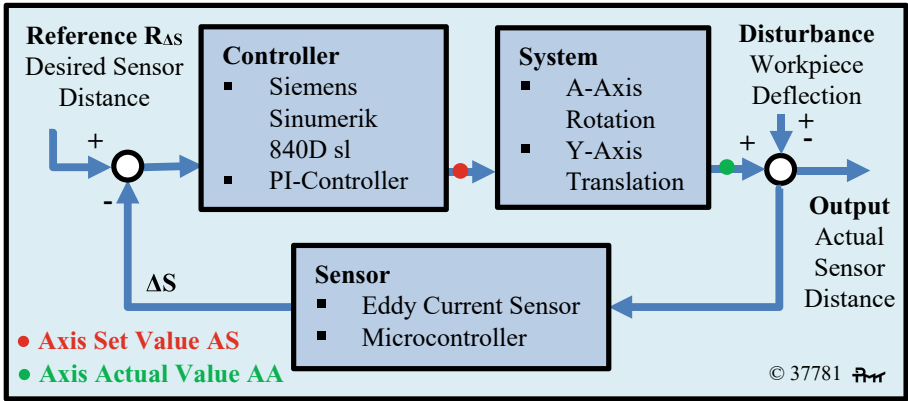


Fig. 1. Control Loop

**Sensor Data Preparation.** The process of peripheral milling involves a discontinuous cut, resulting in cyclic loading. Sensors therefore detect a deflection that fluctuates with the tooth engagement frequency. Since this fluctuation occurs too rapidly for the machine to compensate, it represents an unwanted disturbance in the signal and needs leveling. This is achieved by using an Arduino Due microcontroller positioned downstream of the eddy current sensor. The microcontroller calculates a moving average over the approximate tooth engagement wavelength  $\lambda_z \approx 10$  ms before passing the signal to the PI-controller. By averaging the sensor data over this period, the rapid fluctuations are smoothed out, providing a stable signal for the feedback loop.

**PI-Controller.** The variable to be controlled is the distance  $\Delta S$  measured by the eddy current sensors. Comprising the system to be controlled are the translational Y-axis and the rotational A-axis of the machining center, shown in Fig. 2. Before the machining trials, the sensors are positioned at an arbitrary distance within their measuring range  $S_R = 2.0$  mm, and the necessary reference workpiece-sensor-distance  $R_{\Delta S}$  to achieve the desired wall thickness is calculated. For example, with a desired wall thickness  $t_d = 2.2$  mm, a tool radius  $R_T = 8.0$  mm, and sensors-tool-rotation-axis-distance  $S_d = 12.0$  mm, the desired sensor distance amounts to  $R_{\Delta S} = 1.8$  mm.

**Y-Axis Control.** The control of additional width of cut  $a_e$  via Y-axis feed is based on the deviation between the reference distance  $R_{\Delta S2}$  and the actual distance  $\Delta S_2$  of one sensor. An additional Y-axis set value  $AS_Y$  required is calculated by the PI-controller, which adjusts the axis until the reference and actual value matches.

**A-Axis Control.** The control of additional inclination  $\xi$  via A-axis feed is based on the difference between the actual distances  $\Delta S_1$  and  $\Delta S_2$  of the two sensors. Using the difference in distances and the vertical separation of the sensor positions  $L_s = 14$  mm, as illustrated in Fig. 2, an angle  $\alpha$  is calculated. The PI-controller calculates an additional A-axis set value  $AS_A$  needed and adjusts the axis to bring  $\alpha$  back to  $0^\circ$ . Rotation is executed around the tool center point using the Siemens Sinumerik function TRAORI.

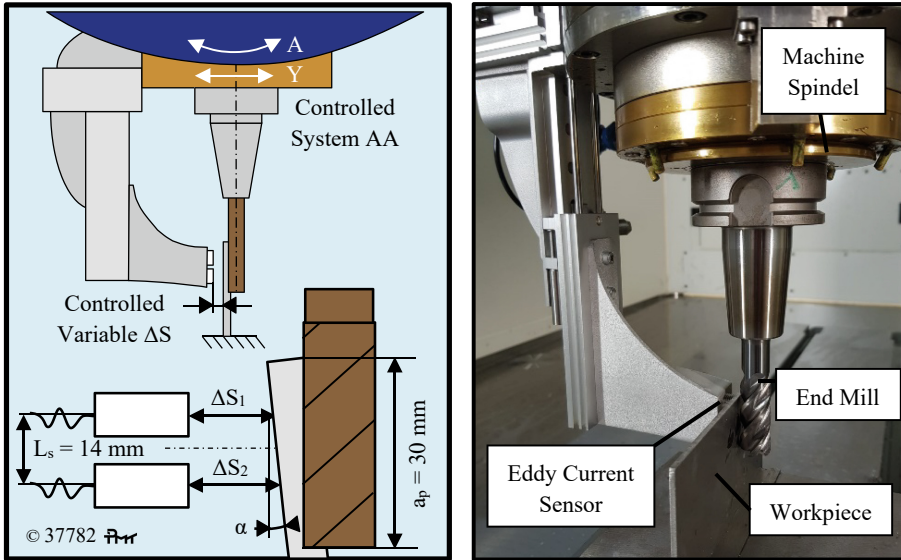


Fig. 2. Test Setup

**PI-Gains.** The proportional and integral PI-controller gains  $K_{PR}$  and  $T_n$  were experimentally determined using the Ziegler-Nichols method. Following this, the integral time constant was manually adjusted to prevent excessive overshooting. This adjustment was necessary due to a high delay time  $T_u = 70$  ms of the control loop, which resulted in poor controllability. Additionally, low maximum compensation speeds otherwise led to an integral windup effect.

**System Compensation Speeds.** The additional axis set values  $AS_A$  and  $AS_Y$  calculated by the PI-controller are transmitted to the machine. Due to the increased mechanical load on the tool by increasing feed and chip thickness, the speed at which the machine executes the set values gets limited. For achieving the desired additional width of cut  $a_e$  via Y-axis, the maximum feed rate has been limited to  $v_f = 20$  mm/min. Similarly, the maximum feed rate to increase the inclination  $\xi$  via A-axis feed has been limited to  $v_A = 38^\circ$ /min. Consequently, the axis actual additional values  $AA_A$  and  $AA_Y$  lag behind the axis set values  $AS_A$  and  $AS_Y$  of the PI-controller. Maintaining these controlled compensation speeds helps prevent undue stress and wear on the tool.

### 3 Test Setup

Experiments were conducted on a FOOKE ENDURA 711LINEAR 5-axis machining center. The workpiece was a cantilevered wall made of Ti-6Al-4V Grade 5, featuring a thickness of approximately  $t \approx 2.6$  mm, a length of  $l = 125$  mm, and a height of  $h = 60$  mm. Using a solid carbide end mill with a diameter  $D = 16$  mm, the workpiece was machined to a target width of  $t_t = 2.2$  mm with two axial depths of cut  $a_p = 30$  mm, following the process parameters depicted in Fig. 3. Six experimental series were

conducted, as listed in Table 1. Next to comparing the presented control loop system with a conventional machining approach, the method gets compared using a worn tool with width of wear mark  $VB = 70 \mu\text{m}$ . To further demonstrate the current challenges with conventional strategies for machining compliant parts, two additional experimental series were conducted. After the first machining pass, an “air cut” was performed on the same tool path without further radial width of cut  $a_e$  to remove any excess material left behind. This strategy was executed with both double and triple passes.

**Table 1.** Test Series

Tool Condition	Milling Method	Repetitions
New	With Control Loop	3
New	Conventional	1
Worn	With Control Loop	1
Worn	Conventional	1
New	Conventional & 1x “air cut”	1
New	Conventional & 2x “air cut”	1

During the machining with the control loop, the feedback system was activated after machining length  $L_M = 10 \text{ mm}$  and deactivated after machining length  $L_M = 115 \text{ mm}$ . The PI-controller axis set values  $AS_A$  and  $AS_Y$ , as well as the actual axis values  $AA_A$  and  $AA_Y$  of the system, were recorded using the Siemens Sinumerik Trace function. Subsequently, the resulting surface profile was measured using a MarSurf XR 20 / GD 120 tactile measure instrument, and the maxima of the wall thicknesses were measured using an outside micro-meter.

## 4 Results

Figure 3 illustrates the control log, showing that the red PI-controller axis set values  $AS_A$  and  $AS_Y$  increase approximately 1.5 s after machining starts when the system is activated and decrease to zero after approximately 18 s when the system is deactivated. The blue and green actual axis values  $AA_A$  and  $AA_Y$  closely match the set values, showing good PI-controller setup.

At both the beginning and end of the machining process, the compensation values  $AA$  are higher due to the increased wall compliance at these points, with maximum inclination  $\xi = 1.2^\circ$  at  $P1_A$  and additional width of cut  $a_e = 0.4 \text{ mm}$  at  $P1_Y$ . In contrast, the stiffer middle section requires lower compensation values, with inclination  $\xi = 0.9^\circ$  at  $P2_A$  and width of cut  $a_e = 0.3 \text{ mm}$  at  $P2_Y$ . Additionally, during the machining of the lower of the two axial depths of cut  $a_p$ , even smaller compensation values are needed with inclination  $\xi = 0.2^\circ$  at  $P3_A$  and width of cut  $a_e = 0.05 \text{ mm}$  at  $P3_Y$ . The system’s adaptation to tool wear is evident when comparing the compensation values used in the worn tool experiment. At  $P4_A$ , the inclination  $\xi = 2.4^\circ$  and at  $P4_Y$  the width of cut  $a_e$

= 0.8 mm show significantly higher compensation compared to the values with the new tool. This demonstrates the system's ability to adjust to changes in tool condition.

#### 4.1 Dimensional Accuracy

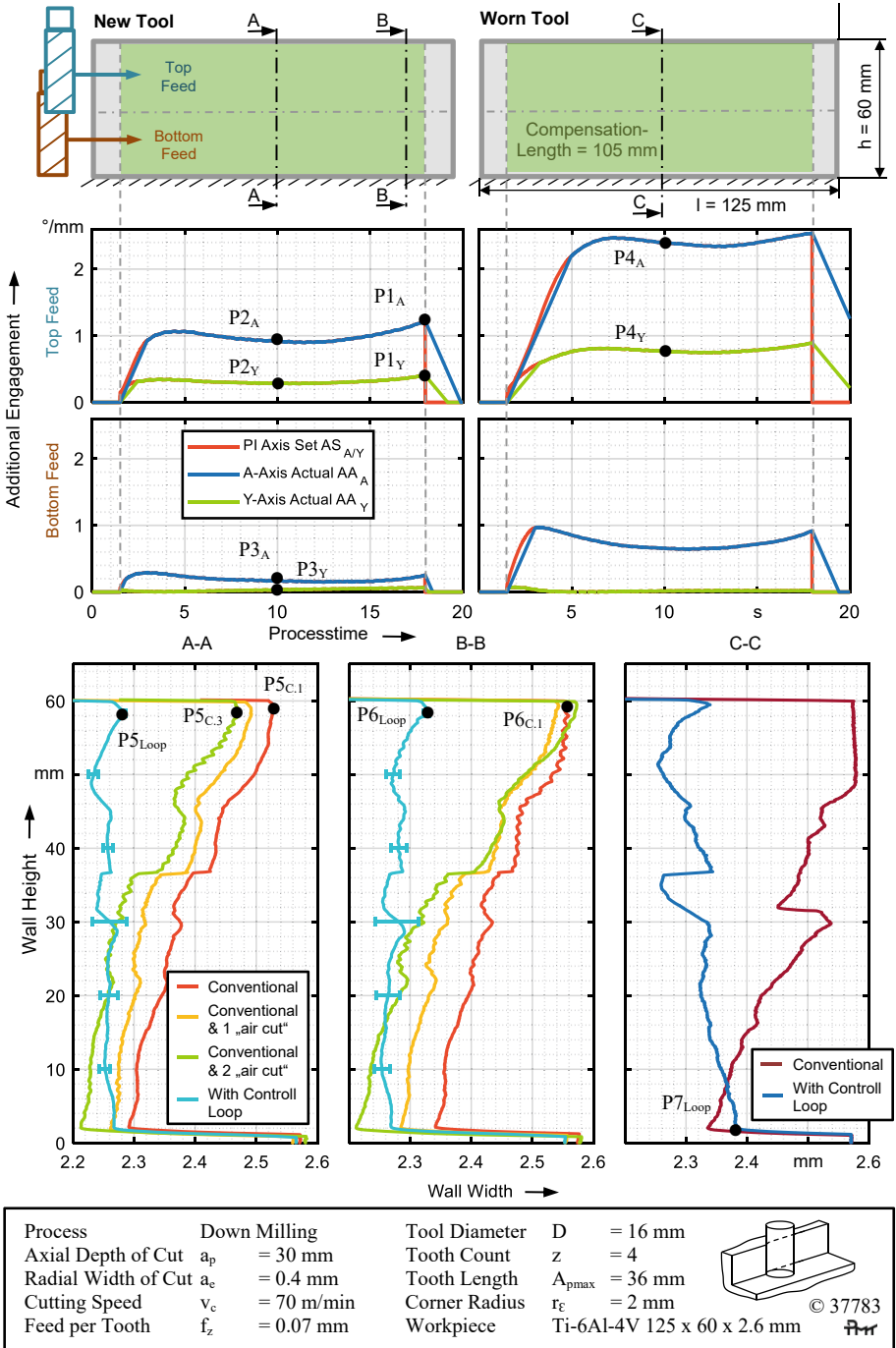
Figure 3 A-A illustrates that with the conventional method, the dimensional error increases with the wall height due to workpiece deflection. The maximum dimensional error at the first pass amounts to  $\Delta D = 330 \mu\text{m}$  at P5<sub>C.1</sub>. By applying a second and third "air cut" pass, this error can be reduced to  $\Delta D = 270 \mu\text{m}$  at P5<sub>C.3</sub>. With the control loop activated, the maximum dimensional error is significantly reduced by 70% to  $\Delta D = 80 \mu\text{m}$  at P5<sub>Loop</sub>. The maximum standard deviation between the 3 repetitions occurs at a wall height of  $h = 30 \text{ mm}$  and amounts to  $SD = 28 \mu\text{m}$ .

Figure 3 B-B shows the dimensional error at machining length  $LM = 110 \text{ mm}$ . The maximum dimensional error without the control loop is  $\Delta D = 360 \mu\text{m}$  at P6<sub>C.1</sub>. A second and third pass are unable to significantly reduce this dimensional error further. With the control loop in place, the maximum dimensional error is reduced by 64% to  $\Delta D = 130 \mu\text{m}$  at P6<sub>Loop</sub>. The maximum standard deviation between the 3 repetitions occurs again at a wall height of  $h = 30 \text{ mm}$  and amounts to  $SD = 35 \mu\text{m}$ .

Figure 3 C-C displays the dimensional error in the middle of the wall when using a worn tool. Machining without the control loop shows that the wall was not machined beyond a height of  $h = 50 \text{ mm}$  due to severe deflection, leaving the wall at its original stock dimension. With the assistance of the control loop, machining continued effectively, and the maximum dimensional error occurred at the lowest point of the wall, with  $\Delta D = 180 \mu\text{m}$  at P7<sub>Loop</sub>, likely due to tool deflection.

#### 4.2 Energy Savings

The findings indicate that machining compliant near-net-shaped thin-walled parts using conventional strategies is very time-consuming or nearly impossible. Even with two "air cuts" to remove excess material left behind after the first tool path, machining at very compliant positions (Fig. 3 B-B) left behind more than 85% of the wall thickness to be machined. This produces excessive machining time, thereby increasing energy, tool and resource consumption, which renders the AM structure unattractive for industrial usage and prevents the potential to reduce the to be machined and downcycled material by up to 95%. The proposed method demonstrates the ability to machine the compliant structures while maintaining high productivity, 66% less machining time and achieving up to 70% less dimensional error compared with the conventional approach. This makes AM structures attractive for industrial use and unlocks the full potential of material and energy savings in AM of thin-walled components.



**Fig. 3.** Trace of the additional system feed & Profile of the dimensional error at various thin wall locations after machining

## 5 Conclusion and Outlook

A method for milling thin-walled structures was presented in the study, which records process force-induced workpiece deflection and compensates for the resulting dimensional errors through a feedback control system. This system dynamically adjusts the toolpath in terms of radial width of cut  $a_e$  and inclination  $\xi$  to counteract the typically arising dimensional deviations. Consequently, the system automatically adapts to the compliance of the workpiece and tool wear condition. Comparisons with conventional machining strategies demonstrate that the control loop reduces the maximum dimensional error by up to 70% while also reducing the machining time and associated energy and resource consumption by more than 66%. This advancement enables the effective machining of highly compliant parts, rendering AM for thin-walled parts more attractive for industrial usage. As a result, the full potential to reduce the to be machined and downcycled material of AM by up to 95% for thin-walled parts can be realized.

Future research should focus on the influence of different sensor positions, sensor data preparation methods, compensation speeds, PI-parameters and tools on compensation quality. Additionally, incorporating tool deflection into the compensation strategy offers significant potential for further dimensional error reduction [12].

**Acknowledgments.** The authors gratefully acknowledge the financial support of the Federal Ministry for Economic Affairs and Climate Action, Ministerium für Wirtschaft und Klimaschutz (BMWK) within the research project AMAvia, PNO 20W1902F.

## References

1. Herranz, S., et al.: The milling of airframe components with low rigidity: a general approach to avoid static and dynamic problems. *Proc. Inst. Mech. Engineers Part B: J. Eng. Manuf.* **219**(11), 789–801 (2005)
2. McDonald, D.T., Luo, P., Palanisamy, S., Dargusch, M.S., Xia, K.: Ti-6Al-4V recycled from machining chips by equal channel angular pressing. *Key Eng. Mater.* **520**, 295–300 (2012)
3. Alexander, I., Vladimir, G., Petr, P., Mihail, K., Yuriy, I.: Machining of thin-walled parts produced by additive manufacturing technologies. *Procedia CIRP* **41**, 1023–1026 (2016)
4. Budak, E., Altintas, Y.: Modeling and avoidance of static form errors in peripheral milling of plates. *Int. J. Mach. Tools Manuf* **35**(3), 459–476 (1995)
5. Scippa, A., Grossi, N., Campatelli, G.: FEM based cutting velocity selection for thin walled part machining. *Procedia Cirp* **14**, 287–292 (2014)
6. Del Sol, I., Rivero, A., López de Lacalle, L.N., Gamez, A.J.: Thin-wall machining of light alloys: A review of models and industrial approaches. *Materials* **12**(12), 2012 (2019)
7. Lassila, A.A., Svensson, D., Wang, W., Andersson, T.: Numerical evaluation of cutting strategies for thin-walled parts. *Sci. Rep.* **14**(1), 1459 (2024)
8. Wimmer, S.S.: *Prognose und Kompensation von Formabweichungen bei der Fräsbearbeitung dünnwandiger Strukturen.* utzverlag GmbH, München (2020)
9. Ratchev, S., Liu, S., Becker, A.A.: Error compensation strategy in milling flexible thin-wall parts. *J. Mater. Process. Technol.* **162**, 673–681 (2005)
10. Huang, N., Yin, C., Liang, L., Hu, J., Wu, S.: Error compensation for machining of large thin-walled part with sculptured surface based on on-machine measurement. *Int. J. Adv. Manuf. Technol.* **96**, 4345–4352 (2018)

11. Liu, H., et al.: State-space theory–based closed-loop control of machining error of thin-walled part modeling and application. *Int. J. Adv. Manuf. Technol.* **127**, 1721–1735 (2023)
12. Ma, W., et al.: Multi-stage error compensation with closed-loop quality control in five-axis flank milling of sculptured surface. *Int. J. Adv. Manuf. Technol.* **133**, 2891–2906 (2024)

**Open Access** This chapter is licensed under the terms of the Creative Commons Attribution 4.0 International License (<http://creativecommons.org/licenses/by/4.0/>), which permits use, sharing, adaptation, distribution and reproduction in any medium or format, as long as you give appropriate credit to the original author(s) and the source, provide a link to the Creative Commons license and indicate if changes were made.

The images or other third party material in this chapter are included in the chapter's Creative Commons license, unless indicated otherwise in a credit line to the material. If material is not included in the chapter's Creative Commons license and your intended use is not permitted by statutory regulation or exceeds the permitted use, you will need to obtain permission directly from the copyright holder.

